Pergamon

Applied Thermal Engineering Vol. 17, No. 3, pp. 211–221, 1997

PII: S1359-4311(96)00041-5
1359-4311/97 $17.00 + 0.00

THERMODYNAMIC DESIGN DATA AND OPTIMUM DESIGN MAPS FOR ABSORPTION REFRIGERATION SYSTEMS

Da-Wen Sun

Department of Agricultural and Food Engineering, University College Dublin, National University of Ireland, Earlsfort Terrace, Dublin, 2, Ireland

(*Received* 5 *August* 1996)

Abstract—Absorption refrigeration systems increasingly attract research interests. The most common cycles are $LiBr/H_2O$ and H_2O/NH_3 absorption machines which have served as standards for comparison in studying and developing new cycles and new absorbent/refrigerant pairs. In the present study, up-to-date thermodynamic properties for $LiBr/H_2O$ and H_2O/NH_3 solution are compiled and are used in cycle simulation. Detailed thermodynamic design data and optimum design maps are presented. These results form a source of reference for developing new cycles and searching for new absorbent/refrigerant pairs. They can also be used in selecting operating conditions for existing systems and achieving automatic control for maintaining optimum operation of the systems. Copyright © 1996 Elsevier Science Ltd.

Keywords—Absorption, air-conditioning, aqua–ammonia, computer simulation, design data, design maps, heat pump, lithium bromide–water, optimisation, refrigeration, water–ammonia, $LiBr–H_2O$, $H_2O–NH_3$.

NOTATION

COP	coefficient of performance
f	flow ratio
h	enthalpy
P	pressure
Q	thermal energy
X	ammonia mass fraction in liquid phase, lithium bromide mass fraction
$\tilde{X}$	ammonia mole fraction in liquid phase
T	temperature
$\dot{w}$	mass flow rate
Y	ammonia mass fraction in vapour phase
$\tilde{Y}$	ammonia mole fraction in vapour phase

Greek letters

ρ	solution density
v	specific volume

Subscripts

a	absorber, absorbent
c	condenser
d	dew point
e	evaporator
g	generator
l	liquid phase of water–ammonia mixture
me	mechanical
re	refrigerant
ss	strong solution (more absorbent, less refrigerant)
v	gas phase of water–ammonia mixture
ws	weak solution (less absorbent, more refrigerant)

INTRODUCTION

In recent years, absorption refrigeration systems have attracted increasing research interest, probably for two reasons. Firstly, the use of ozone-depletion refrigerants can be easily avoided and, secondly, these systems can be powered by waste thermal energy or renewable energies and thus

reduce the demand for electricity. The most common absorption systems are lithium bromide/water ($LiBr/H_2O$) and water/ammonia (H_2O/NH_3) systems, where the components are given as absorbent/refrigerant.

For $LiBr/H_2O$ systems, since water is used as the refrigerant, their application is limited by the freezing point of water and therefore they are usually used in the air-conditioning industry. In contrast, H_2O/NH_3 systems are used in food refrigeration or ice making, since ammonia is the refrigerant. These systems have been studied theoretically [13, 14] and experimentally [7, 8]. In order to improve the performance of absorption systems, new absorbent/refrigerant pairs have been developed. These pairs include $LiBr/H_2O$–NH_3, $LiBr$–$ZnBr_2/CH_3OH$ and $LiNO_3$–KNO_3–$NaNO_3$/H_2O [9], $LiBr$–$ZnBr_2/CH_3OH$ [10], glycerol/H_2O [3], $LiCi/H_2O$ [11] and $NH_3/LiNO_3$ [4]. In these studies, $LiBr/H_2O$ and H_2O/NH_3 pairs were used as standards for comparison. Therefore it is very important that more and accurate information for $LiBr/H_2O$ and H_2O/NH_3 absorption systems is available. In the present study, simulations of $LiBr/H_2O$ and H_2O/NH_3 absorption refrigeration systems are carried out. Detailed thermodynamic design data and optimum design maps are given. It is hoped that these results could serve as a source of reference for designing and selecting new absorption refrigeration systems, developing new absorbent/refrigerant pairs and choosing and optimising suitable operating conditions.

CYCLE DESCRIPTION

The absorption cycle is illustrated in Fig. 1. Low-pressure refrigerant vapour from the evaporator is absorbed by the liquid strong solution in the absorber. The pump receives low-pressure liquid weak solution from the absorber, elevates the pressure of the weak solution and delivers it to the generator. By weak solution (strong solution) is meant that the ability of the solution to absorb the refrigerant vapour is weak (strong) according to ASHRAE definition [2]. In the generator, heat from a high-temperature source drives off the refrigerant vapour in the weak solution. The liquid strong solution returns to the absorber through a throttling valve whose purpose is to provide a pressure drop to maintain the pressure difference between the generator and the absorber. The

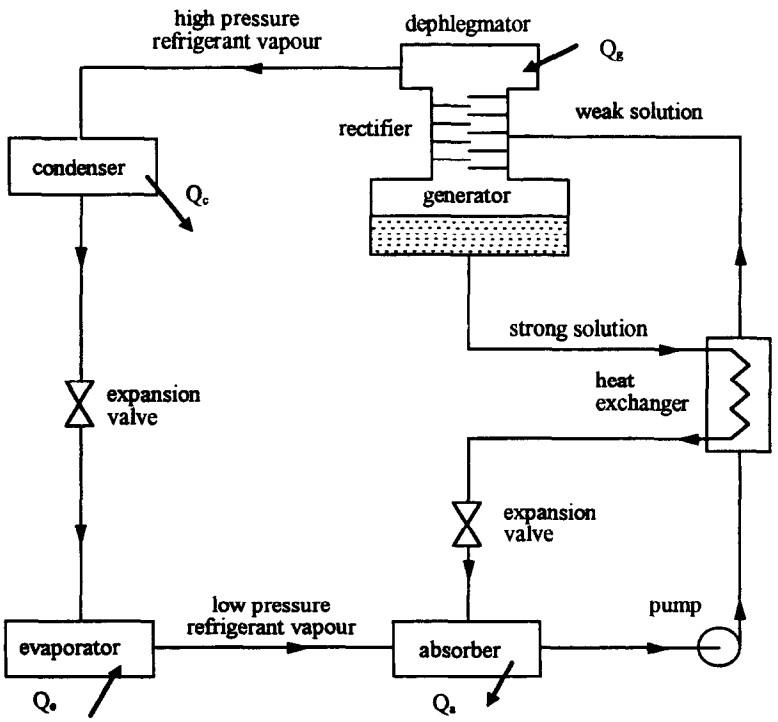

Fig. 1. The schematic of the absorption refrigeration cycle.

high-pressure refrigerant vapour condenses into liquid in the condenser and enters the evaporator through a throttling valve, maintaining the pressure difference between the condenser and the evaporator. In order to improve cycle performance, a solution heat exchanger is normally added to the cycle, as shown in Fig. 1, it is an energy saving component but not essential to the successful operation of the cycle.

The heat flow pattern to and from the four heat exchange components in the absorption cycle is that high-temperature heat enters the generator, while low-temperature heat from the substance being refrigerated enters the evaporator. The heat rejection from the cycle occurs at the absorber and condenser at temperatures such that the heat can be rejected to the atmosphere. The above description is typical for a $LiBr/H_2O$ cycle. However, for the H_2O/NH_3 absorption cycle, it not only consists of all the components previously described, but also a rectifier and dephlegmator, as shown in Fig. 1. The need for the latter two is occasioned by the fact that water is volatile. When ammonia is evaporated off the generator, it also contains some water vapour. When this water enters the evaporator, it elevates the evaporating temperature, it may also freeze along the pipelines. To remove as much water vapour as possible, the vapour driven off at the generator first flows countercurrent to the incoming solution in the rectifier, next, the solution passes through the dephlegmator and condenses some water-rich liquid draining back to the rectifier. By this process, only a small amount of water vapour escapes the dephlegmator and passes from the evaporator to the absorber. It is assumed that the ammonia concentration in the refrigerant is 99%.

The cycle performance is measured by the coefficient of performance (COP), which is defined as the refrigeration rate over the rate of heat addition at the generator plus the work input to the pump, that is

$$\mathrm{COP} = \frac{Q_e}{Q_g + W_{me}} . \tag{1}$$

The mass flow ratio is defined as the mass flow rate of solution from the absorber to the generator (weak solution) to the mass flow rate of working fluid (refrigerant), that is

$$f = \frac{\dot{w}_{ws}}{\dot{w}_{re}} . \tag{2}$$

In order to utilise equation (1), the cycle must be described mathematically, detailed description of various cycles can be found elsewhere [17–21].

SOLUTION PROPERTIES

The thermodynamic properties for $LiBr/H_2O$ and H_2O/NH_3 solutions are pressure, temperature, concentration, enthalpy and density, these properties are interdependent and are necessary for computer simulation of absorption refrigeration systems.

$LiBr/H_2O$ solution

The relation between the solution dew-point temperature (representing saturation pressure) T_d (°F), LiBr concentration X_a (%) and solution temperature T (°F) can be found as follows [16]:

$$T_d(T,X_a) = \sum_{i=0}^{5} \sum_{j=0}^{2} a_{ij} X_a^i T^j . \tag{3}$$

The coefficients in equation (3) are given in Table 1. It should be noted that temperatures in equation (3) are in Fahrenheit, it is easy to convert them into Celsius.

The equation for the LiBr concentration X_a (%), temperature T (°C) and enthalpy (kJ/kg) of $LiBr/H_2O$ solution can be found, with their coefficients given in Table 2, as follows [16]:

$$h(T,X_a) = \sum_{i=0}^{5} \sum_{i=0}^{2} a_{ij} X_a^i T^j . \tag{4}$$

Table 1. Coefficients of equation (3)

i	j	a_{ij}	i	j	a_{ij}	i	j	a_{ij}
0	0	-1.313448×10^{-1}	0	1	9.967944×10^{-1}	0	2	1.978788×10^{-5}
1	0	1.820914×10^{-1}	1	1	1.778069×10^{-3}	1	2	-1.779481×10^{-5}
2	0	-5.177356×10^{-2}	2	1	-2.215597×10^{-4}	2	2	2.002427×10^{-6}
3	0	2.827426×10^{-3}	3	1	5.913618×10^{-6}	3	2	-7.667546×10^{-8}
4	0	-6.380541×10^{-5}	4	1	-7.308556×10^{-8}	4	2	1.201525×10^{-9}
5	0	4.340498×10^{-7}	5	1	2.788472×10^{-10}	5	2	-6.64171×10^{-12}

Table 2. Coefficients of equation (4)

i	j	a_{ij}	i	j	a_{ij}	i	j	a_{ij}
0	0	1.134125	0	1	4.124891	0	2	5.743693×10^{-4}
1	0	-4.80045×10^{-1}	1	1	-7.643903×10^{-2}	1	2	5.870921×10^{-5}
2	0	-2.161438×10^{-3}	2	1	2.589577×10^{-3}	2	2	-7.375319×10^{-6}
3	0	2.336235×10^{-4}	3	1	-9.500522×10^{-5}	3	2	3.277592×10^{-7}
4	0	-1.188679×10^{-5}	4	1	1.708026×10^{-6}	4	2	-6.062304×10^{-9}
5	0	2.291532×10^{-7}	5	1	-1.102363×10^{-8}	5	2	3.901897×10^{-11}

Table 3. Coefficients of equation (5)

i	j	a_{ij}	i	j	a_{ij}	i	j	a_{ij}
0	0	9.939006×10^{-1}	0	1	-5.631094×10^{-4}	0	2	1.392527×10^{-6}
1	0	1.046888×10^{-2}	1	1	1.633541×10^{-5}	1	2	-2.801009×10^{-7}
2	0	-1.667939×10^{-4}	2	1	-1.110273×10^{-6}	2	2	1.734979×10^{-8}
3	0	5.332835×10^{-6}	3	1	2.882292×10^{-8}	3	2	$-4.232988 \times 10^{-10}$
4	0	-3.440005×10^{-8}	4	1	$-2.523579 \times 10^{-10}$	4	2	3.503024×10^{-12}

The relation between the solution density ρ (kg/m^3), temperature T (°C) and LiBr concentration X_a (%) is given, with their coefficients listed in Table 3, as follows [16]:

$$\rho(T,X_a) = \sum_{i=0}^{4}\sum_{j=0}^{2} a_{ij} X_a^i T^j . \tag{5}$$

In equation (3), the solution dew-point temperature is the saturation temperature of steam T (K), which is related to the saturation pressure of steam P (MPa), with coefficients given in Table 4, as follows [12]:

$$P(T) = \exp\left(- \frac{3968.06}{T - 39.5735} + \sum_{i=0}^{9} a_i T^i \right) \tag{6}$$

or

$$T(P) = 42.6776 - \frac{3892.7}{\ln(P) - 9.48654} \quad \text{for } P < 12.33 \text{ MPa} \tag{7a}$$

Table 4. Coefficients of equation (6)

i	a_i	i	a_i
0	1.04592×10^{1}	5	8.6531×10^{-13}
1	-4.04897×10^{-3}	6	9.03668×10^{-16}
2	-4.1752×10^{-5}	7	-1.9969×10^{-18}
3	3.6851×10^{-7}	8	7.79287×10^{-22}
4	-1.0152×10^{-9}	9	1.91482×10^{-25}

Table 5. Coefficients of equation (8)

i	a_i equation (8b)	b_i equation (8c)
1	$8.839230108 \times 10^{-1}$	$4.57874342 \times 10^{-1}$
2	-2.67172935	5.08441288
3	6.22640035	-1.48513244
4	$-1.31789573 \times 10^{1}$	-4.81351884
5	-1.91322436	2.69411792
6	6.87937653×10^{1}	-7.39064542
7	$-1.24819906 \times 10^{2}$	1.04961689×10^{1}
8	7.21435404×10^{1}	-5.46840036

Table 6. Coefficients of equations (10) and (11)

Equation (10)				Equation (11)			
i	m_i	n_i	a_i	i	m_i	n_i	a_i
1	0	0	3.22302	1	0	1	−7.6108
2	0	1	-3.84206×10^{-1}	2	0	4	2.56905×10^{1}
3	0	2	4.60965×10^{-2}	3	0	8	-2.47092×10^{2}
4	0	3	-3.78945×10^{-3}	4	0	9	3.25952×10^{2}
5	0	4	1.3561×10^{-4}	5	0	12	-1.58854×10^{2}
6	1	0	4.87755×10^{-1}	6	0	14	6.19084×10^{1}
7	1	1	-1.20108×10^{-1}	7	1	0	1.14314×10^{1}
8	1	2	1.06154×10^{-2}	8	1	1	1.18157
9	2	3	-5.33589×10^{-4}	9	2	1	2.84179
10	4	0	7.85041	10	3	3	7.41609
11	5	0	-1.15941×10^{-1}	11	5	3	8.91844×10^{2}
12	5	1	-5.2315×10^{-2}	12	5	4	-1.61309×10^{3}
13	6	0	4.89596	13	5	5	6.22106×10^{2}
14	13	1	4.21059×10^{-2}	14	6	2	-2.07588×10^{2}
				15	6	4	−6.87393
				16	8	0	3.50716

Table 7. Coefficients of equations (12) and (13)

Equation (12)				Equation (13)			
i	m_i	n_i	a_i	i	m_i	n_i	a_i
1	0	0	3.24004	1	0	0	1.28827
2	0	1	-3.9592×10^{-1}	2	1	0	1.25247×10^{-1}
3	0	2	4.35624×10^{-2}	3	2	0	−2.08748
4	0	3	-2.18943×10^{-3}	4	3	0	2.17696
5	1	0	−1.43526	5	0	2	2.35687
6	1	1	1.05256	6	1	2	−8.86987
7	1	2	-7.19281×10^{-2}	7	2	2	1.02635×10^{1}
8	2	0	1.22362×10^{1}	8	3	2	−2.3744
9	2	1	−2.24368	9	0	3	−6.70515
10	3	0	-2.0178×10^{1}	10	1	3	1.64508×10^{1}
11	3	1	1.10834	11	2	3	−9.36849
12	4	0	1.45399×10^{1}	12	0	4	8.42254
13	4	2	6.44312×10^{-1}	13	1	4	−8.58807
14	5	0	−2.21246	14	0	5	−2.77049
15	5	2	-7.56266×10^{-1}	15	4	6	-9.61248×10^{-1}
16	6	0	−1.35529	16	2	7	9.88009×10^{-1}
17	7	2	1.83541×10^{-1}	17	1	10	3.08482×10^{-1}

$$T(P) = -387.592 - \frac{12587.5}{\ln(P) - 15.2578} \quad \text{for } P \geq 12.33 \text{ MPa}. \tag{7b}$$

The refrigerant in the $LiBr/H_2O$ system is water, the relations between the saturated temperature T (K) and enthalpies H (kJ/kg) are given as follows, with coefficients listed in Table 5 [12]:

$$T_R = \frac{647.3 - T}{647.3}, \tag{8a}$$

for saturated liquid water;

$$h(T) = 2099.3\left(a_1 + \sum_{i=2}^{8} a_i T_R^{i-1}\right), \tag{8b}$$

for saturated water vapour (steam);

$$h(T) = 2099.3\left(1 + b_1 T_R^{1/3} + b_2 T_R^{5/6} + B_3 T_R^{7/8} + \sum_{i=4}^{8} b_i T_R^{i-3}\right). \tag{8c}$$

Table 8. Coefficients of equation (15)

i	j	a_{ij}	i	j	a_{ij}	i	j	a_{ij}	i	j	a_{ij}
0	0	9.9842×10^{-4}	0	1	3.5489×10^{-4}	0	2	-1.2006×10^{-4}	0	3	3.2426×10^{-4}
1	0	-7.8161×10^{-8}	1	1	5.2261×10^{-6}	1	2	-1.0567×10^{-5}	1	3	9.8890×10^{-6}
2	0	8.7601×10^{-9}	2	1	-8.4137×10^{-8}	2	2	2.4056×10^{-7}	2	3	-1.8715×10^{-7}
3	0	-3.9076×10^{-11}	3	1	6.4816×10^{-10}	3	2	-1.9851×10^{-9}	3	3	1.7727×10^{-9}

Table 9. Derived thermodynamic design data for absorption systems operating on $LiBr/H_2O$

T_g °C	T_c °C	T_a °C	T_e °C	X_{ws} %	X_{ss} %	f	COP	Q_g kW	Q_c kW	Q_a kW	Q_e kW
60.0	20.0	20.0	2.5	49.1	58.4	6.3	0.86	46.88	42.18	45.08	40.38
70.0	20.0	20.0	2.5	49.1	63.0	4.5	0.83	48.82	42.49	46.71	40.38
80.0	20.0	20.0	2.5	49.1	67.4	3.7	0.77	52.13	42.80	49.71	40.38
90.0	20.0	20.0	2.5	49.1	71.8	3.2	0.68	59.05	43.12	56.32	40.38
70.0	30.0	20.0	2.5	49.1	57.9	6.6	0.83	47.57	41.79	45.46	39.68
80.0	30.0	20.0	2.5	49.1	62.4	4.7	0.81	48.86	42.10	46.44	39.68
90.0	30.0	20.0	2.5	49.1	66.6	3.8	0.77	51.75	42.42	49.01	39.68
80.0	40.0	20.0	2.5	49.1	57.4	7.0	0.81	48.33	41.40	45.91	38.98
90.0	40.0	20.0	2.5	49.1	61.8	4.9	0.80	48.86	41.71	46.13	38.98
60.0	20.0	20.0	5.0	46.8	58.4	5.0	0.88	46.19	42.18	44.47	40.46
70.0	20.0	20.0	5.0	46.8	63.0	3.9	0.84	47.99	42.49	45.96	40.46
80.0	20.0	20.0	5.0	46.8	67.4	3.3	0.79	50.97	42.80	48.63	40.46
90.0	20.0	20.0	5.0	46.8	71.8	2.9	0.71	57.13	43.12	54.48	40.46
60.0	30.0	20.0	5.0	46.8	52.9	8.7	0.85	46.55	41.48	44.83	39.76
70.0	30.0	20.0	5.0	46.8	57.9	5.2	0.85	46.77	41.79	44.74	39.76
80.0	30.0	20.0	5.0	46.8	62.4	4.0	0.83	48.06	42.10	45.71	39.76
90.0	30.0	20.0	5.0	46.8	66.6	3.4	0.78	50.67	42.42	48.02	39.76
70.0	40.0	20.0	5.0	46.8	52.4	9.4	0.82	47.60	41.09	45.57	39.05
80.0	40.0	20.0	5.0	46.8	57.4	5.4	0.82	47.38	41.40	45.04	39.05
90.0	40.0	20.0	5.0	46.8	61.7	4.1	0.81	48.09	41.71	45.44	39.05
60.0	20.0	20.0	7.5	44.3	58.4	4.1	0.89	45.59	42.18	43.95	40.54
70.0	20.0	20.0	7.5	44.3	63.0	3.4	0.86	47.23	42.49	45.28	40.54
80.0	20.0	20.0	7.5	44.3	67.4	2.9	0.81	49.89	42.80	47.63	40.54
90.0	20.0	20.0	7.5	44.3	71.8	2.6	0.73	55.34	43.12	52.76	40.54
60.0	30.0	20.0	7.5	44.3	52.9	6.1	0.87	45.54	41.48	43.90	39.84
70.0	30.0	20.0	7.5	44.3	57.9	4.2	0.86	46.10	41.79	44.14	39.84
80.0	30.0	20.0	7.5	44.3	62.4	3.4	0.84	47.33	42.10	45.06	39.84
90.0	30.0	20.0	7.5	44.3	66.6	3.0	0.80	49.67	42.42	47.09	39.84
70.0	40.0	20.0	7.5	44.3	52.4	6.5	0.85	46.28	41.09	44.33	39.13
80.0	40.0	20.0	7.5	44.3	57.4	4.4	0.84	46.61	41.40	44.35	39.13
90.0	40.0	20.0	7.5	44.3	61.8	3.5	0.83	47.40	41.71	44.82	39.13
70.0	20.0	30.0	2.5	55.3	63.0	8.2	0.81	49.61	42.49	47.50	40.38
80.0	20.0	30.0	2.5	55.3	67.4	5.6	0.74	54.76	42.80	52.34	40.38
90.0	20.0	30.0	2.5	55.3	71.8	4.3	0.62	64.69	43.12	61.96	40.38
80.0	30.0	30.0	2.5	55.3	62.4	8.8	0.79	49.94	42.10	47.52	39.68
90.0	30.0	30.0	2.5	55.3	66.6	5.9	0.73	54.03	42.42	51.30	39.68
90.0	40.0	30.0	2.5	55.3	61.8	9.5	0.77	50.92	41.71	48.19	38.98
70.0	20.0	30.0	5.0	53.5	63.0	6.6	0.83	48.73	42.49	46.70	40.46
80.0	20.0	30.0	5.0	53.5	67.4	4.9	0.76	53.35	42.80	51.01	40.46
90.0	20.0	30.0	5.0	53.5	71.8	3.9	0.65	62.33	43.12	59.68	40.46
80.0	30.0	30.0	5.0	53.5	62.4	7.0	0.81	48.99	42.10	46.65	39.76
90.0	30.0	30.0	5.0	53.5	66.6	5.1	0.75	52.72	42.42	50.06	39.76
90.0	40.0	30.0	5.0	53.5	61.7	7.5	0.78	49.75	41.71	47.10	39.05
60.0	20.0	30.0	7.5	51.6	58.4	8.6	0.86	46.89	42.18	45.25	40.54
70.0	20.0	30.0	7.5	51.6	63.0	5.6	0.84	47.98	42.49	46.03	40.54
80.0	20.0	30.0	7.5	51.6	67.4	4.3	0.78	52.14	42.80	49.88	40.54
90.0	20.0	30.0	7.5	51.6	71.8	3.6	0.67	60.27	43.12	57.70	40.54
70.0	30.0	30.0	7.5	51.6	57.9	9.2	0.83	47.79	41.79	45.83	39.84
80.0	30.0	30.0	7.5	51.6	62.4	5.8	0.83	48.24	42.10	45.97	39.84
90.0	30.0	30.0	7.5	51.6	66.6	4.4	0.77	51.61	42.42	49.03	39.84
80.0	40.0	30.0	7.5	51.6	57.4	10.0	0.80	48.84	41.40	46.57	39.13
90.0	40.0	30.0	7.5	51.6	61.8	6.1	0.80	48.86	41.71	46.28	39.13
80.0	20.0	40.0	2.5	60.4	67.4	9.7	0.69	58.61	42.80	56.19	40.38
90.0	20.0	40.0	2.5	60.4	71.8	6.3	0.55	72.90	43.12	70.17	40.38
90.0	30.0	40.0	2.5	60.4	66.6	10.8	0.69	57.23	42.42	54.49	39.68
80.0	20.0	40.0	5.0	58.8	67.4	7.9	0.72	56.19	42.80	53.85	40.46
90.0	20.0	40.0	5.0	58.8	71.8	5.5	0.59	69.10	43.12	66.45	40.46
90.0	30.0	40.0	5.0	58.8	66.6	8.6	0.72	55.00	42.42	52.34	39.76
80.0	20.0	40.0	7.5	57.2	67.4	6.6	0.74	54.47	42.80	52.21	40.54
90.0	20.0	40.0	7.5	57.2	71.8	4.9	0.61	66.13	43.12	63.55	40.54
90.0	30.0	40.0	7.5	57.2	66.6	7.1	0.75	53.44	42.42	50.86	39.84

H_2O/NH_3 solution

The relation between the saturation pressure P (kPa), solution temperature T (K) and ammonia concentration X (decimal) of H_2O/NH_3 mixture is given as [6]

$$\log P = A - \frac{B}{T}\ , \tag{9a}$$

where

$$A = 7.44 - 1.767X + 0.9823X^2 + 0.3627X^3 \tag{9b}$$

$$B = 2013.8 - 2155.7X + 1540.9X^2 - 194.7X^3 . \tag{9c}$$

The relations between the pressure P (kPa), temperature T (K), ammonia concentration $\bar{X},\bar{Y}$ (decimal) and enthalpy (kJ/kg) are as follows [15]. Since for H_2O/NH_3 systems, 1% of water is assumed to exist in the refrigerant, these equations are also used to calculate the thermodynamic properties of the refrigerant.

For the saturated liquid phase (coefficients given in Table 6)

$$T_l(P,\bar{X}) = 100\sum_{i=1}^{14} a_i(1-\bar{X})^{m_i}\left[\ln\left(\frac{2000}{P}\right)\right]^{n_i} \tag{10}$$

$$h_l(T,\bar{X}) = 100\sum_{i=1}^{16} a_i\left(\frac{T}{273.16}-1\right)^{m_i}\bar{X}^{n_i} . \tag{11}$$

For the saturated vapour phase (coefficients given in Table 7)

$$T_v(P,\bar{Y}) = 100\sum_{i=1}^{17} a_i(1-\bar{Y})^{m_i/4}\left[\ln\left(\frac{2000}{P}\right)\right]^{n_i} \tag{12}$$

$$h_v(T,\bar{Y}) = 1000\sum_{i=1}^{17} a_i\left(1-\frac{T}{324}\right)^{m_i}(1-\bar{Y})^{n_i/4} . \tag{13}$$

The relation between the ammonia mole fraction and mass fraction is given by [5]

$$\bar{X} = \frac{17.03X}{17.03X + 18.015(1-X)} . \tag{14}$$

The relation between the specific volume v (m^3/kg), temperature T (°C) and concentration X (decimal) of saturated H_2O/NH_3 solution is fitted by the author with source data taken from the ASHRAE handbook [1] and is given as follows, with the fitted coefficients listed in Table 8:

$$v(T,X) = \sum_{i=0}^{3}\sum_{j=0}^{3} a_{ij}X^jT^i . \tag{15}$$

THERMODYNAMIC DESIGN DATA

In order to provide the thermodynamic design data for absorption refrigeration machines, well established computer software [17–21] is used to simulate the performance of absorption systems against the thermodynamic properties listed in equations (3)–(14). The operating temperature ranges are selected as follows: generator temperature T_g = 60–90°C; condenser temperature T_c = 20–40°C; absorber temperature T_a = 20–40°C; evaporator temperature T_e = 2.5–7.5°C; mass flow rate of refrigerant $\dot{w}_{re}$ = 1.0 kg/s; effectiveness of heat exchanger 0.8.

Tables 9 and 10 list the detailed thermodynamic design data for each combination of the four basic operating temperatures. Table 9 is for the $LiBr/H_2O$ cycle, while Table 10 is for the H_2O/NH_3 cycle. Since the refrigerant rate is chosen to be 1.0 kg/s, the results of heat flow into or from the systems can be scaled up or down according to Tables 9 and 10 for other refrigerant flow rates. These tables can also be used to determine the refrigerant flow rate required for a constant cooling capacity, that is, if the Q_e value is fixed at a certain value, other data can be easily converted. It should be noted that in Tables 9 and 10, X_{ws}, X_{ss}, f and COP are determined by the operating conditions T_g, T_c, T_a and T_e, while Q_g, Q_c, Q_a and Q_e are directly related to the mass flow rate of refrigerant $\dot{w}_{re}$. The values of Q_g, Q_c, Q_a and Q_e approximately determine the sizes of the refrigerators and hence the costs.

Table 10. Derived thermodynamic design data for absorption systems operating on H_2O/NH_3

T_g °C	T_c °C	T_a °C	T_e °C	X_{ws} %	X_{ss} %	f	COP	Q_g kW	Q_c kW	Q_a kW	Q_e kW
60.0	20.0	20.0	2.5	62.4	47.1	3.4	0.80	25.73	21.85	24.43	20.52
70.0	20.0	20.0	2.5	62.4	41.4	2.7	0.78	26.14	21.94	24.73	20.52
80.0	20.0	20.0	2.5	62.4	36.2	2.4	0.77	26.55	21.99	25.10	20.52
90.0	20.0	20.0	2.5	62.4	31.4	2.2	0.76	26.92	21.97	25.48	20.52
60.0	30.0	20.0	2.5	62.4	54.8	5.8	0.74	26.63	21.04	25.38	19.71
70.0	30.0	20.0	2.5	62.4	48.1	3.6	0.74	26.22	21.14	24.85	19.71
80.0	30.0	20.0	2.5	62.4	42.4	2.8	0.74	26.42	21.18	24.99	19.71
90.0	30.0	20.0	2.5	62.4	37.3	2.5	0.74	26.70	21.16	25.28	19.71
70.0	40.0	20.0	2.5	62.4	55.8	6.5	0.67	27.92	20.31	26.64	18.89
80.0	40.0	20.0	2.5	62.4	49.2	3.8	0.70	26.73	20.35	25.35	18.89
90.0	40.0	20.0	2.5	62.4	43.5	2.9	0.71	26.68	20.34	25.29	18.89
60.0	20.0	20.0	5.0	65.4	47.1	2.8	0.82	25.16	21.85	23.93	20.60
70.0	20.0	20.0	5.0	65.4	41.4	2.4	0.80	25.59	21.94	24.26	20.60
80.0	20.0	20.0	5.0	65.4	36.2	2.2	0.79	26.00	21.99	24.62	20.60
90.0	20.0	20.0	5.0	65.4	31.4	2.0	0.78	26.34	21.97	24.99	20.60
60.0	30.0	20.0	5.0	65.4	54.8	4.2	0.77	25.48	21.04	24.29	19.79
70.0	30.0	20.0	5.0	65.4	48.1	3.0	0.77	25.53	21.14	24.23	19.79
80.0	30.0	20.0	5.0	65.4	42.4	2.5	0.77	25.81	21.18	24.45	19.79
90.0	30.0	20.0	5.0	65.4	37.3	2.2	0.76	26.10	21.16	24.76	19.79
70.0	40.0	20.0	5.0	65.4	55.8	4.5	0.72	26.24	20.31	24.99	18.96
80.0	40.0	20.0	5.0	65.4	49.2	3.1	0.73	25.90	20.35	24.57	18.96
90.0	40.0	20.0	5.0	65.4	43.5	2.5	0.73	25.99	20.34	26.68	18.96
60.0	20.0	20.0	7.5	68.7	47.1	2.4	0.84	24.63	21.85	23.47	20.67
70.0	20.0	20.0	7.5	68.7	41.4	2.1	0.82	25.06	21.94	23.80	20.67
80.0	20.0	20.0	7.5	68.7	36.2	1.9	0.81	25.44	21.99	24.14	20.67
90.0	20.0	20.0	7.5	68.7	31.4	1.8	0.80	25.76	21.97	24.47	20.67
60.0	30.0	20.0	7.5	68.7	54.8	3.2	0.80	24.68	21.04	23.54	19.86
70.0	30.0	20.0	7.5	68.7	48.1	2.5	0.80	24.92	21.14	23.68	19.86
80.0	30.0	20.0	7.5	68.7	42.4	2.2	0.79	25.23	21.18	23.94	19.86
90.0	30.0	20.0	7.5	68.7	37.3	2.0	0.78	25.51	21.16	24.24	19.86
60.0	40.0	20.0	7.5	68.7	64.1	7.7	0.70	26.93	20.22	25.91	19.04
70.0	40.0	20.0	7.5	68.7	55.8	3.4	0.75	25.17	20.31	23.97	19.04
80.0	40.0	20.0	7.5	68.7	49.2	2.6	0.75	25.18	20.35	23.92	19.04
90.0	40.0	20.0	7.5	68.7	43.5	2.2	0.75	25.35	20.34	24.10	19.04
60.0	20.0	30.0	2.5	53.8	47.1	7.8	0.75	27.36	21.85	26.09	20.52
70.0	20.0	30.0	2.5	53.8	41.4	4.6	0.75	27.18	21.94	25.79	20.52
80.0	20.0	30.0	2.5	53.8	36.2	3.6	0.74	27.52	21.99	26.08	20.52
90.0	20.0	30.0	2.5	53.8	31.4	3.0	0.73	27.91	21.97	26.48	20.52
70.0	30.0	30.0	2.5	53.8	48.1	9.0	0.67	29.08	21.14	27.78	19.71
80.0	30.0	30.0	2.5	53.8	42.4	5.0	0.71	27.89	21.18	26.49	19.71
90.0	30.0	30.0	2.5	53.8	37.3	3.7	0.71	27.90	21.16	26.50	19.71
80.0	40.0	30.0	2.5	53.8	49.2	10.8	0.59	31.53	20.35	30.30	18.89
90.0	40.0	30.0	2.5	53.8	43.5	5.4	0.66	28.69	20.34	27.36	18.89
60.0	20.0	30.0	5.0	56.0	47.1	5.9	0.78	26.30	21.85	25.08	20.60
70.0	20.0	30.0	5.0	56.0	41.4	4.0	0.78	26.52	21.94	25.20	20.60
80.0	20.0	30.0	5.0	56.0	36.2	3.2	0.76	26.94	21.99	25.57	20.60
90.0	20.0	30.0	5.0	56.0	31.4	2.8	0.75	27.35	21.97	26.00	20.60
70.0	30.0	30.0	5.0	56.0	48.1	6.5	0.72	27.39	21.14	26.13	19.79
80.0	30.0	30.0	5.0	56.0	42.4	4.2	0.73	27.05	21.18	25.71	19.79
90.0	30.0	30.0	5.0	56.0	37.3	3.3	0.73	27.23	21.16	25.90	19.79
80.0	40.0	30.0	5.0	56.0	49.2	7.4	0.66	28.77	20.35	27.53	18.96
90.0	40.0	30.0	5.0	56.0	43.5	4.4	0.68	27.62	20.34	26.34	18.96
60.0	20.0	30.0	7.5	58.3	47.1	4.6	0.81	25.52	21.85	24.37	20.67
70.0	20.0	30.0	7.5	58.3	41.4	3.4	0.80	25.93	21.94	24.67	20.67
80.0	20.0	30.0	7.5	58.3	36.2	2.8	0.78	26.39	21.99	25.09	20.67
90.0	20.0	30.0	7.5	58.3	31.4	2.5	0.77	26.81	21.97	25.52	20.67
70.0	30.0	30.0	7.5	58.3	48.1	5.0	0.75	26.28	21.14	25.07	19.86
80.0	30.0	30.0	7.5	58.3	42.4	3.6	0.75	26.33	21.18	25.06	19.86
90.0	30.0	30.0	7.5	58.3	37.3	2.99	0.75	26.61	21.16	25.35	19.86
80.0	40.0	30.0	7.5	58.3	49.2	5.5	0.70	27.16	20.35	25.95	19.04
90.0	40.0	30.0	7.5	58.3	43.5	3.7	0.71	26.75	20.34	25.53	19.04
70.0	20.0	40.0	2.5	46.9	41.4	10.4	0.70	29.32	21.94	27.97	20.52
80.0	20.0	40.0	2.5	46.9	36.2	5.9	0.71	28.69	21.99	27.27	20.52
90.0	20.0	40.0	2.5	46.9	31.4	4.4	0.71	28.87	21.97	27.46	20.52
90.0	30.0	40.0	2.5	46.9	37.3	6.4	0.66	29.64	21.16	28.28	19.71
70.0	20.0	40.0	5.0	48.7	41.4	7.8	0.74	27.90	21.94	26.61	20.60
80.0	20.0	40.0	5.0	48.7	36.2	5.0	0.74	27.91	21.99	26.55	20.60
90.0	20.0	40.0	5.0	48.7	31.4	3.9	0.73	28.24	21.97	26.89	20.60
80.0	30.0	40.0	5.0	48.7	42.4	9.0	0.67	29.50	21.18	28.22	19.79
90.0	30.0	40.0	5.0	48.7	37.3	5.4	0.69	28.61	21.16	27.31	19.79
90.0	40.0	40.0	5.0	48.7	43.5	10.5	0.59	31.69	20.34	30.53	18.96
70.0	20.0	40.0	7.5	50.7	41.4	6.2	0.77	26.92	21.94	25.68	20.67
80.0	20.0	40.0	7.5	50.7	36.2	4.3	0.76	27.22	21.99	25.93	20.67
90.0	20.0	40.0	7.5	50.7	31.4	3.5	0.75	27.64	21.97	26.36	20.67
80.0	30.0	40.0	7.5	50.7	42.4	6.8	0.71	27.99	21.18	26.76	19.86
90.0	30.0	40.0	7.5	50.7	37.3	4.6	0.71	27.76	21.16	26.51	19.86
90.0	40.0	40.0	7.5	50.7	43.5	7.7	0.65	29.34	20.34	28.19	19.04

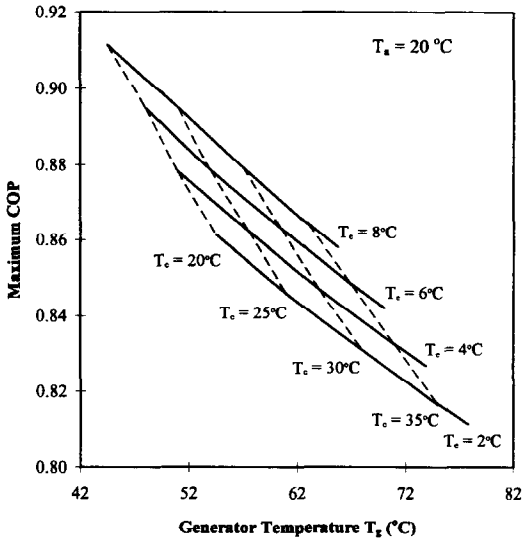

Fig. 2. The optimum design map for absorption systems operating on LiBr/H_2O with absorber temperatures at 20°C.

OPTIMUM DESIGN MAPS

It is understood that for absorption systems, their COP values illustrate the local maximum for various operating conditions [17–21]. The COP values shown in Tables 9 and 10 are the values a system can achieve at the specified conditions; however, they are not necessarily optimum values, in other words, the specified operating conditions are not optimised. Therefore, some energy is wasted.

In order to provide detailed optimum operating conditions for absorption systems, the computer software [17–21] was used to search for different operating conditions with which an absorption cycle reaches its maximum performance. These results are constructed as optimum design maps and are shown in Figs 2 – 5. Among them, Figs 2 and 3 are for LiBr/H_2O cycles with one map for $T_a = 20°C$ and the other for $T_a = 30°C$, and Figs 4 and 5 for H_2O/NH_3 cycles with one map

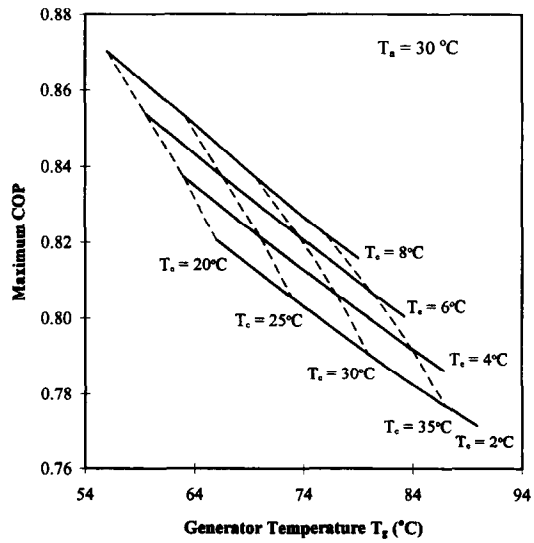

Fig. 3. The optimum design map for absorption systems operating on LiBr/H_2O with absorber temperatures at 30°C.

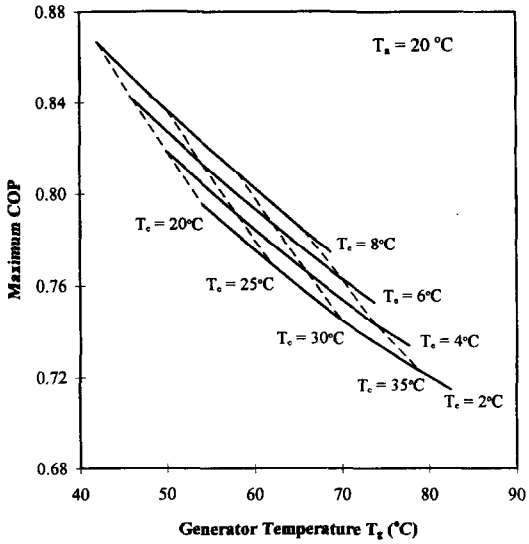

Fig. 4. The optimum design map for absorption systems operating on H_2O/NH_3 with absorber temperatures at 20°C.

for $T_a = 20°C$ and the other for $T_a = 30°C$. In these Figures, the dashed lines represent constant condenser temperatures and solid lines for evaporator temperatures. If T_e, T_c and T_a are specified, from the maps, T_g can be found and, under these conditions, COP can also be found from the maps. This COP is the maximum value. If one of the temperatures shifts away, the cycle COP will be lower than the original maximum COP, and the conditions are no longer optimised unless other conditions are readjusted according to the maps. Taking Fig. 2 as an example, if $T_e = 4°C$, $T_c = 30°C$ and $T_a = 20°C$, from the map, T_g can be found to be 64°C and COP is 0.847, which is maximum. If T_g shifts to 58°C, from Table 9 by interpolation, the new COP value is 0.836, which is lower than the original optimum value of 0.847 and hence indicates that new conditions are not optimised. In order to maintain optimum operation, for $T_g = 58°C$, T_c must be decreased to 25°C along the solid line of $T_e = 4°C$ in Fig. 2 if the refrigerating temperature is required to be kept constant and, in this case, the conditions are optimised again and the COP value is 0.862, as indicated in the map. Again this value is higher than the non-optimum value of 0.836.

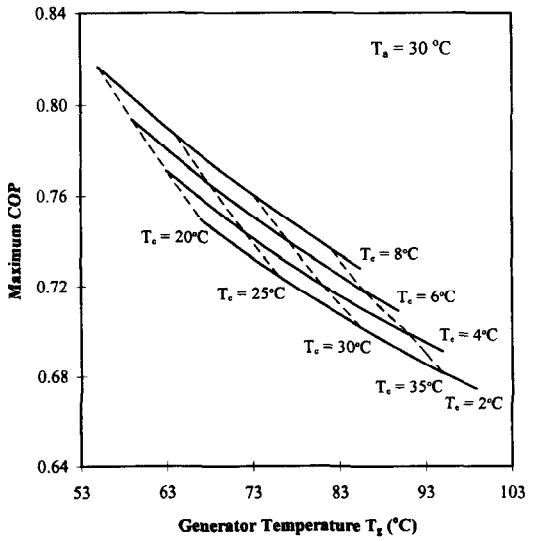

Fig. 5. The optimum design map for absorption systems operating on H_2O/NH_3 with absorber temperatures at 30°C.

These optimum design maps are very important in designing new systems, choosing operating conditions for existing systems. They can also be stored in computers to realise automatic control of absorption systems for maintaining their optimum operation under various operating conditions.

CONCLUSIONS

Detailed thermodynamic design data and optimum design maps for the most common $LiBr/H_2O$ and H_2O/NH_3 absorption refrigeration cycles are presented. The results are calculated using well established simulation software, based on up-to-date thermodynamic properties of $LiBr/H_2O$ and H_2O/NH_3 solutions.

It is hoped that these results can serve as a source of reference for comparison in developing new cycles and new absorbent/refrigerant pairs. These results can be used to select operating conditions for $LiBr/H_2O$ and H_2O/NH_3 absorption refrigeration machines and to realise automatic control for maintaining optimum operation of these systems under different conditions.

REFERENCES

1. ASHRAE, Refrigerant properties. In 1993 *ASHRAE Handbook*, *Fundamentals*, Chapter 17, p. 17.81. ASHRAE, Atlanta (1993).
2. ASHRAE, Absorption cooling, heating, and refrigeration equipment. In 1994 *ASHRAE Handbook*, *Refrigeration Systems and Applications*, Chapter 40, p. 40.1. ASHRAE, Atlanta (1994).
3. N. Bennani, M. Prevost and A. Coronas, Absorption heat pump cycle: performance analysis of water–glycerol mixture. *Heat Recovery Systems & CHP* **9**(3), 257–263 (1989).
4. R. Best, L. Porras and F. A. Holland, Thermodynamic design data for absorption heat pump systems operating on ammonia–lithium nitrate: part I. Cooling. *Heat Recovery Systems & CHP* **11**(1), 49–61 (1991).
5. M. Bogart, *Ammonia Absorption Refrigeration in Industrial Processes*. Gulf, Houston, Texas (1981).
6. P. Bourseau and R. Bugarel, Absorption–diffusion machines: comparison of the performances of NH_3–H_2O and NH_3–NaSCN. *Int. J. Refrig.* **9**, 206–214 (1986).
7. D. Butz and K. Stephan, Dynamic behaviour of an absorption heat pump. *Int. J. Refrig.* **12**, 204–212 (1989).
8. M. A. R. Eisa and F. A. Holland, A study of the performance parameters in a water–lithium bromide absorption cooler. *Energy Res.* **10**, 137–144 (1986).
9. G. Grossman and K. Gommed, A computer model for simulation of absorption systems in flexible and modular form. *ASHRAE Trans.* **93**(2), 2389–2427 (1987).
10. G. S. Grover, M. A. R. Eisa and F. A. Holland, Thermodynamic design data for absorption heat pump systems operating on water–lithium chloride: part I. Cooling. *Heat Recovery Systems & CHP* **8**(1), 33–41 (1988).
11. P. D. Iedema, Simulation of stationary operation and control of a $LiBr/ZnBr_2/CH_3OH$ absorption heat pump system. In *Directly Fired Heat Pump—for Use in Domestic and Commercial Premises*, *Proc. of Int. Conf*, University of Bristol, Edited by P. W. Fitt and R. T. Moses, Paper No. 2.1. University of Bristol, UK (1984).
12. T. F. Irvine and T. Uemura, *Steam and Gas Tables with Computer Equations*. Academic Press, New York (1984).
13. S. C. Kaushik and S. C. Bhardwaj, Theoretical analysis of ammonia–water absorption cycles for refrigeration and space conditioning systems. *Energy Res.* **6**, 205–225 (1982).
14. D. A. Kouremenos and E. D. Rogdakis, Thermodynamic cycles for refrigeration and heat transformer units H_2O/LiBr. *Forshung im Ingenieurwesen* **54**(2), 39–47 (1988).
15. J. Patek and J. Klomfar, Simple functions for fast calculations of selected thermodynamic properties of the ammonia–water system. *Int. J. Refrig.* **18**(4), 228–234 (1995).
16. M. R. Patterson and H. Perez-Blanco, Numerical fits of the properties of lithium–bromide water solutions. *ASHRAE Trans.* **94**(2), 2059–2077 (1988).
17. D.-W. Sun, Computer simulation and optimisation of ammonia–water absorption refrigeration systems. *Energy Sources* (in press) (1997).
18. D.-W. Sun, The aqua–ammonia absorption system—an alternative option for food refrigeration. *J. Food Engng* (in press), (1997).
19. D.-W. Sun, Comparison of the performances of NH_3–H_2O, NH_3–$LiNO_3$ and NH_3–NaSCN absorption refrigeration systems. *Energy Convers. Mgmnt* (in press), (1997).
20. D.-W. Sun and I. W. Eames, Performance characteristics of HCFC-123 ejector refrigeration cycles. *Int. J. Energy Res.* **20**(10), 871–885.
21. D.-W. Sun, I. W. Eames and S. Aphornratana, Evaluation of a novel combined ejector–absorption refrigeration cycle. I. Computer simulation. *Int. J. Refrig.* **19**(3), 172–180.